A-337 - Rpt #7(Final)
Contract: DA19-129-qm-1487
Northwestern University

Mechanisms of Freeze Dehydration

Period: 29 September 1959 - 28 December 1961

QUARTERMASTER FOOD AND CONTAINER INSTITUTE FOR THE ARMED FORCES
Research and Engineering Command
Quartermaster Corps, U.S. Army
Chicago, Illinois

CONTRACT RESEARCH PROJECT REPORT

QUARTERMASTER FOOD AND CONTAINER INSTITUTE FOR THE ARMED FORCES, CHICAGO
QM Research and Engineering Command, U. S. Army, QM Research and Engineering Center, Natick, Massachusetts

Northwestern University
Evanston, Illinois

Official Investigator:
Dr. J. Edward Sunderland
Collaborators: J. D. Bannister
N. Koumoutsos
H. L. Miller
V. Sevcik

Project Nr.: 7-84-06-032
Contract: DA19-129-qm-1487
Report Nr.: 7(Final)
File Nr.: A-337
Period: 29 September 1959 -
28 December 1961
Initiation Date: 29 September 1959

Title of Contract: Mechanisms of Freeze Dehydration

INVESTIGATION INTO THE MECHANISM OF FREEZE DRYING

Final Technical Report

INTRODUCTION

The work which has been carried out under this contract is divided into three categories: measurements of the emissivity of beef, measurements of the thermal conductivity of beef, and studies of the mechanism of freeze drying.

1.0 PART I EMISSIVITY OF BEEF

1.1 SUMMARY

The total normal emissivity of lean beef, beef fat, and freeze dried beef has been measured. For a temperature range of 66 F to 94 F, the emissivities of all substances varied between .73 and .78.

The instrument used for the measurements is described. The accuracy of the instrument changes with temperature, but for the temperature range used it is accurate within $\pm$ 4%.

1.2 INTRODUCTION

In calculating the heat transfer by radiation between different surfaces, it is necessary to know the temperatures, areas, and emissivities of the surfaces. Although radiant heat transfer calculations are frequently needed in various food processes involving beef, information concerning the emissivity of beef has not previously been available.

Emissivities are difficult to measure, especially at low temperatures. This is due to the fact that radiation fluxes from surfaces at low temperatures are extremely small and consequently difficult to measure. For this reason, experimental techniques which have been developed for use at high temperatures cannot be used in the low temperature range. Therefore, special equipment has been designed and built to measure the total normal emissivity of meat at temperatures which are of interest in food processing. The method of measuring emissivity described in this paper is similar to the method described by Schmidt (1)*.

---

* Numbers in parenthesis refer to references listed at the end of the report.

1.3 DESCRIPTION OF APPARATUS

1.3.1 General description. The apparatus (Fig. 1) used for measuring the emissivity consists of three major components: a detector; a reference body; and a black body. The detector generates an emf which is dependent on the difference between the radiant energy emitted by the reference body and the energy emitted by either the black body or the sample. The reference body serves as a radiant heat source of known magnitude. The black body serves two purposes. During calibration, it is used as a radiant heat source of known magnitude. When measuring the emissivity, the sample holder is screwed into the black body, and the black body is then used to control the temperature of the sample holder and the sample. The temperature of the black body and the reference body is controlled by circulating a liquid through the annular regions shown in Fig. 1.

1.3.2 The detector. A thermopile made from #36 B & S gauge chromel-constantan wire is used for a detector. The junctions of the thermopile are connected to small copper disks and the entire unit is suspended inside the cylinder as shown in Fig. 2. The outside surfaces of the disks are covered with a lampblack-waterglass coating so that they will absorb most of the incident radiation.

The radiant energy reaching the two collector disks is limited to that which can reach it through two equal solid angles Ω (see Fig. 2). One end of the detector receives radiant energy from the sample and the other end receives radiant energy from the reference body. The detector is suspended inside the reference body by a copper support that also serves the purpose of maintaining the temperature of the detector at the same level as that of the reference body.

1.3.3 The reference body. The reference body consists of a hollow cylinder surrounded by an annular region through which a liquid flows. The temperature of the reference body is controlled by varying the temperature of the liquid. The inner cylinder is made out of 4 in. ID copper pipe with .250 in. thick walls and is approximately 11 in. long. An 8N thread (8 threads per inch) has been turned on the inside of the cylinder. The bottom of the cylinder is made of 3/8 in. copper plate. A spiral has been cut on the inside face

of the plate to produce a surface similar to the surface of the cylinder walls. The bottom is brazed to the inside cylinder to insure good heat transfer and a uniform temperature. All inside surfaces are painted with a lampblack-waterglass coating. The outside cylinder is made out of 5 in. brass pipe with .250 in. walls. Baffles are placed between the inner and the outer cylinder walls to guide the coolant and thus insure uniform temperature. The entire assembly is insulated and enclosed in a wooden box to minimize heat losses. The temperature of the inside cylinder is measured by thermocouples at the center of the bottom plate and at a point near the open end. The temperature distribution of the reference body is uniform once steady state conditions are reached.

1.3.4 Black body. The black body is constructed in the same manner as the reference body except that the inside cylinder is approximately 20 in. long. The black body serves two purposes. In the first place, it serves as a black body; i.e., as a standard of radiation. Secondly, it serves to control the temperature of the sample. That is, it cools or warms the sample holder which in turn keeps the sample at any desired temperature. The sample holder is made of copper and is screwed into the black body to provide intimate thermal contact with the black body. The meat sample is placed inside the sample holder and is in contact with the copper holder along the edges and the bottom. With this arrangement it is possible to maintain a uniform sample temperature. To make sure that the detector "sees" only the sample, the geometry is arranged so that only the center portion of the sample is visible to the detector. The temperature of the meat is measured with fine thermocouples threaded in the meat and located just below the surface. When the sample holder is unscrewed, the detector is able to "see" the inside surfaces of the cylinder which can then be used for calibration purposes. The temperature of the black body is measured by a thermocouple in the center of the bottom disk and another one about half way up the cylinder wall. An analysis similar to the ones described by Buckley (2) and Daws (3) and Rossman (4) shows that the apparent emissivity of the black body is greater than .9976.

1.4 THEORETICAL ANALYSIS

The primary mode of heat transfer to the detector disks is radiation.

For this type of measurement Schmidt (1) and Snyder et al (5) show that the emissivity of the sample can be caluclated from the relation

$$\epsilon_s = \frac{EC}{T_s^4 - T_r^4} \qquad (1)$$

where E is the output of the detector, C is a calibration constant, T_s and T_r are the absolute temperatures of the sample and reference bodies respectively.

In order to determine the calibration constant C, the sample is removed so that the detector has a direct view of the black body. Thus, with this arrangement $\epsilon_s = 1$, and from Eq. 1,

$$C = (T_b^4 - T_r^4) / E \qquad (2)$$

where T_b is the absolute temperature of the black body. It is interesting to note that if the black body and the sample are at the same temperature, and if the temperature of the reference body is constant, then the emissivity is given by

$$\epsilon_s = \frac{E_{sample}}{E_{black\ body}} \qquad (3)$$

where E_{sample} is the output of the detector with the sample in place, and $E_{black\ body}$ is the output of the detector with the black body in place.

1.5 EXPERIMENTAL PROCEDURE

Equation 1 shows that the emissivity of any sample can be determined from knowledge of the output of the detector, the temperature of the sample, the temperature of the reference body, and the constant C. The constant C is measured by placing the black body under the open end of the reference body. The heating and cooling liquids are then pumped

through the apparatus and once steady state conditions are reached, the temperatures of the reference and black bodies are measured, and the output of the detector is measured with a galvanometer. The value of C can be determined from Eq. 2. Once the constant C is determined, the sample holder is screwed into the black body and the sample is placed inside the sample holder. After steady state conditions are established, the thermopile output and the temperatures of the reference body and the sample are measured. From this data, the emissivity can be determined using Eq. 1.

All meat and fat samples are cut with a hack-saw from a large frozen piece of beef. The samples are cut in a direction normal to the fibers. The surfaces are scraped clean and the samples are thawed. The samples are 3.5 in. in diameter and 0.5 in. thick. The temperatures of the samples are measured with two #36 B & S gauge copper-constantan thermocouples, one in the center of the sample and one near its edge. The thermocouples are threaded through the meat and fat samples just slightly below the surface in order to measure the actual surface temperatures as closely as possible. Since the temperatures of the reference and the black bodies are also measured by copper-constantan thermocouples, all the thermocouples are connected to a common reference junction which is kept at 32 F. Although these thermocouples are not calibrated, they have been matched; that is, more thermocouples have been made than are actually required, and only those that give the same reading for one particular condition have been selected.

1.6 RESULTS

The value of the constant C was measured at various temperatures and was found to equal 1.03. To test the accuracy, the emissivity of a thick lampblack-waterglass coat on brass and the emissivity of asbestos paper was measured. The values measured are compared to measurements reported by Schmidt (1) and McAdams (6) (see Fig. 3).

The emissivity of the following meat and fat samples have been measured.

a. Three samples of lean beef at approximately 94 F.
b. Two samples of lean beef at approximately 70 F.
c. One sample of lean beef at approximately 80 F.
d. Two samples of freeze-dried lean beef at approximately 66 F. These samples were freeze-dried for over 48 hours until no further loss of weight occurred.
e. Two samples of beef fat at approximately 94 F.
f. Two samples of beef fat at approximately 70 F.

All beef samples were 69.5% moisture. The emissivity has been determined for the temperature range of 65 to 100 F for the following reasons. The lower limit of 65 F is set by the instrument; below this temperature, condensation of vapor on the detector starts to influence its output. The upper limit of 100 F is set by the samples because above this temperature, the samples start to lose surface moisture very rapidly. When this happens, the surface of the sample becomes very tough and dry-looking. The emissivity of freeze-dried meat is determined only at 70 F because at higher temperatures large temperature gradients occur across the sample. This is attributed to the difficulty of maintaining good thermal contact between the freeze-dried sample and the sample holder. The experimental results are given in Fig. 3.

1.7 CONCLUSIONS

As seen from Fig. 3, the emissivity of lampblack-waterglass and the emissivity of the asbestos paper as determined by this investigation is within about 2% of the published data.

It is interesting to note that within the temperature range studied, the emissivity of both meat and fat decrease with increasing temperature. This variation of emissivity with temperature also occurs with wood and most non-conducting solids.

The fat and meat samples started to lose a considerable amount of moisture when measurements were made at temperatures above about 100 F. After a period of time, the surface would appear dry and tough. To determine what effect, if any, the dry surface has on the emissivity of the sample, one meat sample was left in the apparatus longer than any other sample (2 1/2 hours). This sample had a tough, dry-looking surface for approximately an hour toward the end of the run, yet no difference in emissivity was observed. This seems to indicate that drying of the surface has very little effect on the emissivity. This observation is substantiated by noting that the emissivity of freeze-dried meat is roughly the same as the emissivity of fresh meat (see Fig. 3).

An error analysis based on a method developed by Kline and McClintock (7) shows that the maximum possible error for a single measurement is about $\pm$ 4%. However, since the experimental measurements fall within $\pm$ 2% of the average measured values, and since the measurements of asbestos and lampblack-waterglass fall within 2% of other published data, it is the opinion of the writers that the mean values of the results given in Fig. 3 are accurate to within $\pm$ 2%.

2.0 PART II THERMAL CONDUCTIVITY OF BEEF

2.1 SUMMARY

Measurements of the thermal conductivity of beef muscle are presented and compared with published results. The meat samples are taken from an eye of loin, U. S. Good grade. The results apply for heat flow parallel to the grain of the samples. The error of the measurements is estimated to be less than $\pm$ 2.75% of the reported values.

A model is presented which provides a rough estimate of the thermal conductivity of beef for temperatures between 0 and 22 F and for moisture content between 60 and 80%.

2.2 INTRODUCTION

Knowledge of the thermal conductivity of food substances is essential

in order to make analytical studies of transient processes in which such substances are heated, cooled, or dehydrated. Analytical studies of this type are useful for obtaining the optimum design of equipment used for heating, freezing, freeze drying and other methods of dehydrating food products. There are very few substances that undergo transient thermal processes as frequently and on as large a scale as beef; therefore, it is most surprising that very little is known about the thermal conductivity of beef. One object of this report is to present the results of recent measurements of the thermal conductivity of beef and to present a method whereby the thermal conductivity of beef can be estimated for conditions not measured.

The thermal conductivity of beef has been shown to depend on temperature; moisture content; direction of heat transfer with respect to the fiber; and for dehydrated beef, the thermal conductivity also depends on pressure. Although these factors can have a large influence on the thermal conductivity, several early investigators failed to specify them. A summary of thermal conductivity measurements of beef which have been reported by other investigators is given in Table 1. A more complete summary, covering the specific heat and thermal conductivity of beef and other meats is presented by Miller (14).

2.3 APPARATUS

The measurements of thermal conductivity which are given in this report were made with a guarded hot plate which is similar to a hot plate used by the National Bureau of Standards (15). Basically, the hot plate assembly is comprised of two cooling plates and a heater. Two samples are placed in the assembly as shown in Fig. 4. With this arrangement, an equal amount of heat delivered by the heater is conducted through each sample.

The heater plate is made up of two separate units, a primary heater and a guard heater. The primary heater is centrally located and provides the heat flux which is used to calculate the thermal conductivity from

Table 1

Thermal Conductivity of Beef

Reference	Material	% Moisture	Direction of heat flow with respect to the fiber direction	Temp. °F	Conductivity Btu/hr ft °F
Awbery & Griffiths (8)	Beef			-200	.895
Hardy & Soderstrom (9)	Beef Muscle				.114
	Beef Fat				.118
Tappel, et al, (10)	Beef				.130
Cherneeva (11)	Beef, lean	78.5	Perpendicular	32	.277
			Perpendicular	23	.612
			Perpendicular	14	.779
			Perpendicular	-4	.907
	Beef, fat	74.5	Perpendicular	32	.277
			Perpendicular	23	.537
			Perpendicular	14	.692
			Perpendicular	-4	.827
	Beef fat	7		32	.118
				23	.122
				14	.131
				-4	.141
Harper (12)	Beef Muscle Atmos. Press.	Freeze Dried	Parallel	58	.0375
	Beef Muscle .01 mm Hg	Freeze Dried	Parallel	58	.0216
Lentz (13)	Beef, lean flank, 3.4% fat	74	Perpendicular	32	.280
			Perpendicular	23	.588
			Perpendicular	14	.616
			Perpendicular	-4	.675
	Beef, lean Sirloin, 0.9% fat	75	Parallel	32	.284
			Parallel	23	.742
			Parallel	14	.792
			Parallel	-4	.904
	Beef, udder fat, 89% fat	9		23	.166
				14	.148

experimental data. The guard heater surrounds the primary heater; the two heaters are separated by a 1/8 inch air gap. The power input to each heater is adjusted so that there is a negligible temperature difference across the gap; therefore, the edge heat loss from the primary heater is negligible. The temperature difference between the primary and guard heaters is measured by a 32 junction thermopile, which is made from 30 BS gage chromel and constantan wire. Chromel-constantan wires are used because this combination gives a higher emf than other common thermocouple materials.

The cooling plates consist of copper tubing labyrinths which are soldered to 1/4 inch copper plates; solder is built up around the tubing to provide good thermal contact. A mixture of ethylene glycol and water from a constant temperature bath is pumped through the tubing at about one gallon per minute.

Because thermistors are more sensitive than thermocouples, they are used to measure the temperature of the hot and cold plates.

2.4 PROCEDURE

The beef samples for this investigation are taken from the eye of loin, U. S. Good grade. The meat as delivered is freshly cut, and then it is aged for two weeks in a high humidity room at 36 F. The samples are frozen in a home freezer; the samples are not permitted to thaw, except the samples used to measure the conductivity above the freezing point. No measurements are taken on refrozen samples. The samples are weighed to determine losses in moisture during storage and testing. For this investigation there is no measurable loss of moisture. At the conclusion of the tests, the moisture content of each sample is determined by freeze drying. The samples are considered dry when there is no change in weight over an 8 hour period.

Due to the large size of the primary heating area, it is necessary to piece the samples together from four or five smaller pieces. The fiber of the meat is aligned so that the thermal conductivity is measured with heat flow parallel to the fiber. The samples are then

frozen and run through a planer to produce a flat surface.

The samples are then placed in the hot plate apparatus with the surfaces of the hot and cold plates wetted to provide good thermal contact. Furthermore, in order to minimize thermal contact resistances, a compressive force is applied to the samples by tightening four corner bolts between the top and bottom cold plates.

After the samples are in place, the apparatus is covered with two inches of fiber glass insulation as required by ASTM Designation C177-45T (15). The ambient air temperature is lowered by placing dry ice in the enclosure containing the hot plate assembly. The ambient air temperature is usually a few degrees above the temperature of the cold plates.

For each measurement, after steady-state conditions are obtained, readings are taken at half hour intervals over a four hour period. The thermal conductivity of a test is then calculated by averaging the conductivities given by the eight sets of readings. At least two tests are performed for each mean temperature; more tests are run if the results differ by more than 1 %. The reported thermal conductivity is then calculated by averaging the results of two or more tests.

2.5 EXPERIMENTAL ACCURACY

An analysis of the experimental accuracy shows that the error in the results is less than $\pm$ 2.7% of the reported values. The magnitude of the error is determined by analyzing instrument errors, errors due to small temperature unbalances between the guard and primary heaters, and errors resulting from assuming that the hot and cold plates represent isothermal surfaces.

The total instrument error is the sum of the errors in measuring the sample thickness, the primary heater area, the heat flux through the sample, and the temperature difference across the sample. An outline of the procedure used in determining the instrument error follows.

The thermal conductivity (k) is calculated from Fourier's law for

heat transfer (q) through a slab of area A and thickness ΔX. Thus

$$k = -\frac{q\Delta X}{A\Delta T} \tag{4}$$

Where ΔT is the temperature difference across the slab. From Eq. 4 it can be seen that

$$k = f(q, A, \Delta X, \Delta T)$$

Differentiating,

$$dk = \frac{\partial f}{\partial q}\,dq + \frac{\partial f}{\partial(\Delta X)}\,d(\Delta X) + \frac{\partial f}{\partial A}\,dA + \frac{\partial f}{\partial(\Delta T)}\,d(\Delta T)$$

Where

$$\frac{\partial f}{\partial q} = -\frac{(\Delta X)}{A(\Delta T)} \qquad \frac{\partial f}{\partial A} = \frac{q(\Delta X)}{A^2(\Delta T)}$$

$$\frac{\partial f}{\partial(\Delta X)} = -\frac{q}{A(\Delta T)} \qquad \frac{\partial f}{\partial(\Delta T)} = \frac{q(\Delta X)}{A(\Delta T)^2}$$

Now by letting the differentials dk, dq, d (ΔX), dA and d (ΔT) take on small incremental values δk, δq, $\delta(\Delta X)$, $\delta(A)$, and $\delta(\Delta T)$ respectively and dividing the left hand side by k and the right hand by $-\frac{q\Delta X}{A\Delta T}$, it can be shown that

$$\text{MAXIMUM ERROR} = \pm\left[\left|\frac{\delta q}{q}\right| + \left|\frac{\delta(\Delta X)}{\Delta X}\right| + \left|\frac{\delta A}{A}\right| + \left|\frac{\delta(\Delta T)}{\Delta T}\right|\right] \tag{5}$$

Woodside and Wilson (16) show that the magnitude of the error in the thermal conductivity due to small temperature unbalances between primary and guard heaters can be expressed by:

$$\frac{\Delta k}{k} = \frac{\Delta X}{A}\,\frac{\Theta}{\Delta T}\left(\frac{q_e}{k} + C\right) \tag{6}$$

That is, the error in the conductivity measurement is a function of the temperature unbalance (Θ), the temperature difference between hot and

cold plates, the sample thickness, the sample conductivity, and two plate constants (q_o) and (C). The plate constants are determined experimently and depend upon the size and design of the heater plate. The plate constants for the heater plate used in this investigation are $q_o = 0.30 \frac{Btu}{hr\,^oF}$ and C = 4.24 ft.

The error in assuming that the hot and cold plates represent isothermal surfaces is determined by estimating the maximum temperature deviation from the mean temperature of the surface. If the thermistors on the hot and cold plates are located so that they measure this maximum deviation from the mean temperature, the maximum error is realized in measuring the temperature across the sample.

An error can result from the thermal contact resistances between the samples and the hot and cold plates. For example, an air gap of 0.024 inches causes an error of 1%. This error is minimized by wetting the surfaces of the hot and cold plates and by applying a compressive force to the samples in the apparatus.

From the above analysis it can be shown that for the experiments reported, the instrument errors total 2.25%, the unbalance error is 0.16%, and the error in assuming that the hot and cold plates are isothermal surfaces is 0.34%. The sum of these errors is ($\pm$) 2.75%.

As an additional check of the accuracy, measurements of the thermal conductivity of two samples of known thermal conductivity are compared with measurements made elsewhere. The first sample, Foamglas* is furnished by the Pittsburgh Corning Corporation and is reported to have a thermal conductivity of 0.394 B/hr.ft.^{o}F. The second sample, a semi-rigid glass fiberboard furnished by the National Bureau of Standards, is reported to have a thermal conductivity of 0.214 $\pm$ 2% B/hr.ft.^{o}F. The values of thermal conductivity measured in this investigation agree within 0.5% and 1.35% with the values given above for Foamglas and fiberboard samples respectively.

---

* Foamglas is the trade name for a rigid cellular glass insulation.

From the analysis presented, it can be concluded that the experimental results are within $\pm$ 2.75% of the actual value. From the results of the measurements of the thermal conductivity of Foamglas and fiberboard, it is very likely that the error is less than $\pm$ 2.75%. In fact, it is possible that the experimental error is within $\pm$ 1% of the reported measurements.

2.6 RESULTS AND EXTROPLATION OF RESULTS

Figure 5 shows the experimental results of this investigation for the thermal conductivity of beef muscle. The sample is aligned so that the heat flow is parallel to the fiber of the meat; the moisture content of the meat is 69.5%. Above the freezing point, the conductivity increases with an increase in temperature. Below freezing, the conductivity varies inversely with temperature. This variation of thermal conductivity with temperature follows the same trend as the thermal conductivity of ice and water.

Between 22 and 32 F, the experimental data is not conclusive because in this range the percentage of meat frozen varies with temperature. More reliable data in this range could be obtained by using small temperature differences between the primary and guard heaters in order to minimize variations of thermal conductivity throughout the sample. It should be noted, however, that the accuracy of the hot plate decreases when the temperature difference between the hot and cold plates is lowered. It is estimated that at about 31 F the amount of moisture frozen and hence also the thermal conductivity vary abruptly with temperature.

The data presented by Lentz (13) is also given in Fig. 5. His results are higher than the results of this investigation; this may be attributed to the higher moisture content (75%) of his samples.

In order to extrapolate the experimental results of the thermal conductivity of beef muscle for different moisture content, the model

shown in Fig. 6 can be used. The model is made up of fibers arranged parallel and normal to the heat flow path; the remaining space is assumed to be filled with water or ice. The model has three parallel paths for heat transfer. The first path is composed only of fibers; the second path is water (or ice); the third path is a series arrangement of water (or ice) and fibers. It is assumed that no energy crosses the boundaries between the paths and that heat is transferred only by thermal conduction. The equivalent electrical circuit of the three paths is shown in Fig. 7.

Consider an area equal to P^2 which lies in a plane perpendicular to the direction of heat transfer (see Fig. 6). If the total sample thickness is ΔX, the thickness of each layer of fibers (P) equals $\frac{\Delta X}{n}$, where n is the number of fiber layers. The temperature drop across each layer of fibers is $\frac{\Delta T}{n}$, where ΔT is the temperature difference across the sample. The rate of heat conduction through the fibers (q_1) is given by

$$q_1 = k_f d(2P - d) \frac{\Delta T}{nP}$$

where k_f is the thermal conductivity of the fibers. The rate of heat conduction through the water and/or ice (q_2) is

$$q_2 = k_w \left[(P-d)^2 - 2d(P-d)\right] \frac{\Delta T}{nP} = k_w \left[P^2 - 4Pd + 3d^2\right] \frac{\Delta T}{nP}$$

where k_w is the thermal conductivity of the water or ice. The rate of heat conduction through the water and/or ice in series with the fiber is given by

$$q_3 = k_{fw} \left[2d(P-d)\right] \frac{\Delta T}{nP}$$

where

$$k_{fw} = \frac{4 k_f k_w}{\frac{d}{P} k_w + \left(4 - \frac{d}{P}\right) k_f}$$

The apparent thermal conductivity, k_a, is given by

$$k_a = \frac{q_1 + q_2 + q_3}{P^2 \frac{\Delta T}{\Delta X}}$$

Therefore, it follows that

$$k_a = k_f \left[2 \frac{d}{P} - \left(\frac{d}{P}\right)^2\right] + k_w \left[1 - 4 \frac{d}{P} + 3\left(\frac{d}{P}\right)^2\right]$$

$$+ \frac{8 k_f k_w \left[\frac{d}{P} - \left(\frac{d}{P}\right)^2\right]}{\frac{d}{P} k_w + \left(4 - \frac{d}{P}\right) k_f} \qquad (7)$$

The volume of one of the cubes (V_T) of the model is given by the sum of the fiber volume (V_f) and the water volume (V_w). That is,

$$V_T = V_f + V_w = P^3$$

From Fig. 6 it can be seen that

$$V_f = 2dP^2 - \frac{1}{2} d^2 P - \frac{d^3}{2}$$

Since d is very small compared with P, the last term of the previous equation can be neglected. Therefore,

$$\frac{d}{P} = 2 - \sqrt{4 - \frac{2V_f}{V_T}} \qquad (8)$$

The negative sign must be used in front of the square root because $\frac{d}{P}$ is always less than one.

Since the density of fresh meat ($63 \frac{lb}{ft^3}$) is nearly equal to the density of the fiber shown in the model ($64.2 \frac{lb}{ft^3}$), they are assumed equal. The ratio $\frac{d}{P}$ can then be expressed in terms of the total

weight and the fiber weight.

Thus

$$\frac{d}{P} = 2 - \sqrt{4 - 2\frac{W_f}{W_T}}$$

Results of calculations of the thermal conductivity based on the model are compared with experimental data for meat with 69.5% and 75% water (see Fig. 5). Harper and Chichester(12) report the thermal conductivity of meat fiber to be $0.0216 \frac{BTU}{hr.ft.\ F}$; in this report, the thermal conductivity of the fiber is assumed to be independent of temperature. The moisture in the meat is assumed to be a 0.28 M salt solution. The variation of thermal conductivity with temperature of a 0.25 M salt solution has been reported by Long (17) and is shown in Fig. 5.

Between OF and 22F, the thermal conductivity calculated by using the model is in close agreement with experimental results for beef with 69.5% moisture. The largest deviation from experimental data occurs in the freezing range where the apparent conductivity of the model is less than the measured values. Above freezing, the experimental results are lower than the values predicted by the model.

For a moisture content of 75%, the values of thermal conductivity predicted by the model are 11% lower than the measurements made by Lentz (13) for the temperature range 0 to 22F. Above freezing, the model indicates values of conductivity which are 20% lower than measured values.

The model presented is useful only for predicting thermal conductivities parallel to the grain. The model is not applicable for meat when the moisture content is less than 60%. As the moisture content decreases, the ratio $\frac{d}{P}$ increases and the assumption that d is small compared to P does not hold and equations (7) and (8) are no longer valid. Furthermore, for a moisture content below 30%, the model predicts a value of thermal conductivity which is negative.

In summary, the model is useful for predicting the thermal conductivity of beef in a direction parallel to the fiber and for beef with a moisture content of 60% or higher.

3.0 PART III THE MECHANISM OF FREEZE DRYING

3.1 SUMMARY

An analysis of the transfer of heat and vapor in a piece of meat which is being freeze dried is presented. Analytical approximations for the rate of drying are given and the results of an experimental investigation of the transient temperature and pressure distributions during freeze drying are presented.

3.2 INTRODUCTION

Sublimation drying or freeze drying, is a technique whereby a moisture containing substance is frozen, placed in a low pressure environment and the moisture is removed by sublination. When organic substances are dehydrated in this manner, they display many properties greatly superior to those dehydrated by conventional methods where the moisture is driven off by heating at atmospheric pressure. A notable result is that many foodstuffs when re-hydrated after sublimation drying, compare favorably with those preserved by freezing. This implies that during the low temperature removal of moisture, the evaporation of normally volatile substances which contribute to the taste and nourishment qualities of a product is arrested. Further, since the product is frozen into its original size and shape prior to and during the moisture removal, the shrinkage effect, and hence appearance deterioration, is minimal.

The great advantage of foodstuffs preserved by freeze-dehydration over those preserved by freezing lies in the transportation and storage consideration. Freeze dried foods require only vacuum packing and no refrigeration, and because of the high moisture content of most foods, there is a weight saving of 50 to 80 percent over frozen products.

To take advantage of these desirable properties of freeze dried foodstuffs for commercial applications, it is necessary to know the

mechanisms governing the process. The following text will discuss these mechanisms as they are applied to beef muscle. The material is divided into two parts; first, a mathematical analysis of the heat and vapor transport; and second, experimental results.

Prior to discussing these two factors it will be advantageous to delineate clearly the character of the process to be considered. We are concerned with the freeze drying of a semi-rigid organic substance, namely beef muscle, which must be handled in bulk. When such a fibrous material is frozen, small ice spears grow between the fibers compressing and dehydrating them. Freeze drying of such a frozen product consists primarily of subliming these ice spears and transporting the vapor and out of the product.

To greatly simplify the drying process a one dimensional model is considered. The model, shown in Fig. 8, consists of a sample placed in a low pressure environment with heat for sublimation added by a radiating heater. It is apparent that except in the earliest stages of drying, heat and vapor transport must take place in opposite directions through a wall of dried product. The drying process can then be visualized as the motion of a subliming front advancing into the frozen material leaving dried material in its wake, through which both the heat of sublimation and the evolved vapor must be transported.

A complete description of the proposed model of a sublimation drying process would incorporate biological considerations. It is believed that an engineering study can be more useful if conducted independently of biological factors insofar as they do not influence the mechanisms of the process. If a comprehensive understanding of the process from an engineering viewpoint can be developed, then the necessary compromises with the biological factors can be made with a knowledge of their influence on the mechanics of the process. The following analysis and description of experimental work will be carried out in the light of this predominantly mechanical model.

3.3 ANALYSIS

3.3.1 General remarks

Before attempting an analysis in mathematical form, it is important to have a clear concept of the variables involved and the results desired. Referring to Fig. 8, it may be seen that the velocity of the subliming interface through the frozen medium is the dependent variable of interest. Thus, we are seeking an expression for this interface velocity, which is proportional to the subliming rate. As shown by Harper and Tappel (18), the independent variables are the temperature at the subliming interface (defining the vapor pressure at the interface), the total pressure, and the vapor pressure at the exterior surface of the dried layer.

We must now place a restriction on one variable, namely, the interface temperature. The surface of dried organic material, when overheated, tends to glaze and form a vapor impeding crust. Thus, there is a maximum temperature to which the product surface may be raised. Harper and Tappel (18) indicate that this temperature is about 100° F for beef muscle. In the interests of obtaining fast drying rates, the heat rate must be maximized, and hence the surface temperature must be held as high as possible but below the glazing temperature. We will assume that this surface temperature is fixed at the optimum value, thereby making the subliming interface temperature no longer independent but dependent on the total and partial pressure ac the product surface.

Summarizing, we will consider the exterior surface temperature to be constant at the optimum value and, hence, the interface velocity to be dependent on the total pressure and the water vapor partial pressure at the exterior surface.

The process is sufficiently slow that a reasonable approximate analysis may be obtained by considering it to be quasi-steady with respect to transients in the temperature and pressure distributions.

Therefore, in this report, steady state equations are used to describe the heat and vapor fluxes at any particular time.

3.3.2 Heat transfer

The instantaneous rate of heat conduction per unit area at any point in the dried layer is given by

$$q'' = -K \frac{\partial T}{\partial x} \tag{9}$$

The term k is the thermal conductivity of the dried meat with water vapor uniformly distributed throughout its pores. If the transfer of energy due to the moving vapor is neglected, and if the thermal conductivity is constant, then Eq. (9) can be integrated to give

$$q'' = \frac{K}{S} (T_o - T_s) \tag{10}$$

where S is the distance between the free surface and the subliming front, T_o and T_s are the temperatures at the free surface and the subliming surface respectively. Equation (10) gives a transient heat flux in terms of an assumed steady state temperature distribution, in accordance with our assumption of quasi-steady temperature and pressure distributions. The transient nature of Eq. (10) occurs because both s and T_s are dependent on time.

It is important to recognize that the thermal conductivity varies both with temperature and the amount of water vapor present in the pores. Furthermore, ice or water entrained in the fibers increase the thermal conductivity. Another factor affecting heat transfer is the heat exchange between the moving vapor and the hot dried lattice. A simple calculation shows that the ratio of the sensible heat required to raise the temperature of water vapor 120° F, to the latent heat of sublimation, is very small. In the absence of experimental data to the contrary, it is assumed that both effects are negligible and that Eq. (10) is valid.

The freeze-drying model illustrated in Fig. 8 lends itself to being represented by a bundle of capillary tubes oriented parallel to the heat and vapor fluxes. For normal freezing times of 1 to 2 hours, Luyet (19) reports that the diameter of the channels in freeze-dried beef muscle is on an average 0.15 mm. He also reports that the cross-sectional area of the channels is 72% of the total area. This data is used to describe our model as a bundle of capillary tubes of diameter 0.15 mm and porosity of 0.72.

The following discussion is similar to the analysis given by Harper and Tappel (18), where the vapor transport is considered as taking place in three possible regimes.

(a) Diffusion.

(b) Hydrodynamic flow.

(c) Combined diffusion and hyrdodynamic flow.

(a) Diffusion

If no total pressure gradient exists between the subliming interface and the exterior surface, the vapor efflux diffuses through a stagnant gas and the dried fiber lattice. Under this condition, the water vapor partial pressure gradient provides the driving force.

A good analysis of simultaneous vapor diffusion and heat transfer in the same direction through a porous wall is given by Glaser (20). He argues that the vapor pressure in the wall cannot exceed the saturation pressure corresponding to the wall temperature because the lateral pore dimension is insufficient to support such a pressure difference. For the case of vapor transport and heat transfer in opposite directions, the pressure and temperature profiles must be divergent from the saturation values, and Glaser would consider the mechanisms as independent. Then the vapor flux per unit area (w) by diffusion is given by

$$W = -\frac{D}{\eta R T} \cdot \frac{d P_w}{d x} \tag{11}$$

Where D in the diffusion coefficient, P_w is the partial pressure of the water vapor, R is the perfect gas constant, and η is a resistance of the dried layer to vapor diffusion. Assuming that the

temperature gradient in the dried section is linear, and that thermal equilibrium exists between the vapor and the lattice, Eq. (11) may be integrated to give

$$w = - \frac{2D}{\eta R (T_o + T_s)} \cdot \left(\frac{P_{ws} - P_{wo}}{S} \right) \quad (12)$$

Where P_{ws} and P_{wo} are the partial pressures of the subliming surface and the free surface respectively, and S is the distance of the subliming surface from the free surface. In performing this integration, it is assumed that D and η are independent of partial pressure.

(b) Hydrodynamic flow

To study the hydrodynamic flow regime, consider a capillaric model previously described by Scheidegger (21). The Hagen-Poiseuille equation for flow in a capillary tube is

$$\frac{dp}{dx} = - 32 \frac{\mu V}{a^2} \quad (13)$$

where u is the viscosity V is the average velocity of the vapor and a is the average capillary diameter. If a unit area of the dried layer is comprised of n capillaries, the vapor flux (w) is given by

$$w = n \cdot \frac{\pi}{4} a^2 \rho V \quad (14)$$

where ρ is the density of the vapor.

Combining Eq. (13) and (14) and using the perfect gas law,

$$w = - n \frac{\pi}{128} \frac{a^4}{\mu} \frac{p}{RT} \frac{dp}{dx} \quad (15)$$

Again assuming thermal equilibrium between the vapor and the dried lattice, and using the average temperature in Eq. (15),

$$w = - n \frac{\pi}{64} \frac{a^4}{\mu} \frac{p}{R(T_o + T_s)} \frac{dp}{dx}$$

Integrating from the exterior surface to the subliming interface and recognizing that in a dried layer of thickness S, the average length of the capillaries may be r, the vapor flux is given by

$$w = -\frac{n\pi a^4}{128}\,\frac{1}{\mu}\,\frac{1}{R(T_0+T_s)}\,\frac{(p_s^2-p_o^2)}{S}\,\left(\frac{S}{r}\right) \tag{16}$$

Using the definition of porosity P

$$P = \frac{n\pi a^2}{4}\,\left(\frac{r}{S}\right)$$

and defining a tortuosity factor, f,

$$f = \frac{r}{S}$$

Equation (16) may be simplified to

$$w = -\frac{1}{32}\,\frac{a^2}{\mu}\,\frac{P}{f^2}\,\frac{p_s+p_o}{R(T_0+T_s)}\,\frac{p_s-p_o}{S} \tag{17}$$

The negative sign indicates that the vapor flux is in the negative x direction. The porosity may be measured readily while the tortuosity factor, in spite of being physically recognizable, is more nebulous when it comes to measurement. The group $\frac{p_s+p_o}{R(T_0+T_s)}$ in Eq. (17) is immediately identified as the average density of the vapor efflux.

The foregoing analysis has assumed that the vapor flux behaves as a continuum. If the mean-free-path of the vapor molecules (λ) approaches the order of magnitude of the capillary diameter, the collisions between the molecules and the capillary walls outnumber the intermolecular collisions, and this assumption is invalid. Knudsen has established a dimensionless parameter to describe this effect,

$$K_n = \frac{\lambda}{d}$$

where K_n is the Knudsen number and d is a characteristic dimension which in this case represe.ts the average pore diameter. Knudsen used this

parameter to delineate the transition from contimuum to free molecule flow as follows:

$Kn > 2$	Free molecule flow
$Kn < .01$	Continuum flow
$2 > Kn > .01$	Slip or transition flow

The transition flow regime is characterized by slip at the boundaries of an essentially continuum type flow.

If a subliming interface temperature of -20° C is assumed and if no total pressure gradient exists across the dried layer, the Knudsen number ranges from .20 to .33. If the total pressure at the outer surface is reduced to 10 microns of mercury, the Knudsen number ranges from .2 to 30. Thus, the flow is at least partly in the transition and free molecule regimes.

Knudsen's equation for free molecule flow in a bundle of capillaries is

$$W = -\frac{2}{3} n \sqrt{2\pi} \frac{\lambda}{\mu} \left(\frac{s}{r}\right) \cdot a^3 \cdot \frac{P_o + P_s}{R(T_o + T_s)} \cdot \frac{P_s - P_o}{s}$$

Similarly to continuum flow we may introduce porosity and the tortuosity factor, so that

$$W = -\frac{4}{3} \sqrt{\frac{2}{\pi}} \frac{P}{f^2} \frac{\lambda}{\mu} a \frac{P_o + P_s}{R(T_o + T_s)} \cdot \frac{P_s - P_o}{s} \tag{18}$$

For the transition regime Schiedegger (21) suggests combining Eqs. (17) and (18) in the form

$$W = -\frac{a}{\mu} \frac{P}{f^2} \left\{ \frac{a}{32} + \frac{4}{3} \sqrt{\frac{2}{\pi}} \lambda Z \right\} \frac{P_s + P_o}{R(T_o + T_s)} \frac{P_s - P_o}{S} \tag{19}$$

where Z is a proportionality factor called the Adzumi constant and is approximately 0.9 for a single gas.

For the case of small total pressure gradients between the exterior surface and the subliming interface, it is reasonable that both hydrodynamic flow and diffusion are significant. For this type of flow the

superposition is valid and the hydrodynamic and diffusion equations may be added.

3.3.4 Subliming front velocity and drying time

Equation (10) describes the heat flow to the subliming interface and Eqs. (12), (17), (18) and (19) describe the vapor flow from the subliming front for the diffusional, hydrodynamic continuum, free molecule and transition regimes, respectively. The vapor flux and heat flux equations may be coupled by an enthalpy balance at the subliming interface.

$$q = -wL \tag{20}$$

where L is the latent heat of sublimation. It is also recognized that the equations are coupled through the relationship between T_s and p_s. This latter relationship may be put into mathematical form through the Clausius-Clapeyron equation. If we can estimate the temperature of the subliming interface and assume that the solid volume is negligible in comparison with the vapor volume, that the vapor behaves as a perfect gas, and that our estimate of the subliming from temperature is sufficiently accurate that variations in latent heat are negligible, the Clausius-Clapeyron equation may be integrated to give

$$p_s = p_1 \exp\left[\frac{L}{R}\left(\frac{1}{T_s} - \frac{1}{T_1}\right)\right] \tag{21}$$

where T_1 is our estimate of the interface temperature and p_1 is the corresponding vapor pressure.

The subliming interface velocity may be described in terms of the vapor flux

$$\frac{ds}{dt} = -\frac{w}{m} \tag{22}$$

where m is a pseudo density, a measure of the mass of ice per unit volume of frozen product.

With the aid of Eq. (20), (21) and (22), the heat and vapor flow equations may be coupled to give the subliming front velocity in terms of the partial vapor pressure at the exterior surface for each of the vapor transport regimes as follows:

(a) Diffusion regime

$$s^2\left(\frac{ds}{dt}\right)^2 - 2sJ\frac{ds}{dt} + \frac{M}{\rho_o}\left\{\rho_{wo} - \rho_i \exp\left[N\left(\frac{1}{1-N_s\frac{ds}{dt}} - \frac{T_o}{T_i}\right)\right]\right\} = 0$$

(b) Combined diffusion and hydrodynamic continuum regime

$$s^2\left(\frac{ds}{dt}\right)^2 - 2sJ\frac{ds}{dt} + \frac{M}{\rho_o}\left\{\rho_{wo} - \rho_i \exp\left[N\left(\frac{1}{1-N_s\frac{ds}{dt}} - \frac{T_o}{T_i}\right)\right]\right\}$$

$$+ \frac{a}{32}\varphi\left\{\rho_o^2 - \rho_i^2 \exp\left[2N\left(\frac{1}{1-N_s\frac{ds}{dt}} - \frac{T_o}{T_i}\right)\right]\right\} = 0$$

(c) Hydrodynamic slip flow regime

$$s^2\left(\frac{ds}{dt}\right)^2 - 2sJ\frac{ds}{dt} + \left(\frac{a}{32} + \frac{\pi}{3}\sqrt{\frac{2}{\pi}}\lambda\varepsilon\right)\varphi\left\{\rho_o^2 - \rho_i^2 \exp\left[2N\left(\frac{1}{1-N_s\frac{ds}{dt}} - \frac{T_o}{T_i}\right)\right]\right\} = 0$$

(d) Hydrodynamic free molecule regime

$$s^2\left(\frac{ds}{dt}\right)^2 - 2sJ\frac{ds}{dt} + \frac{\pi}{3}\sqrt{\frac{2}{\pi}}\lambda\varphi\left\{\rho_o^2 - \rho_i^2 \exp\left[2N\left(\frac{1}{1-N_s\frac{ds}{dt}} - \frac{T_o}{T_i}\right)\right]\right\} = 0$$

Where

$$J = \frac{T_o k}{mL} \qquad M = \frac{2\alpha k}{\eta R L m^2}$$

$$N = \frac{L}{T_o R} \qquad \varphi = \frac{p}{m^2 f^2}\frac{a}{\mu}\frac{k}{RL}$$

It is assumed that the diffusivity is inversely proportional to the total pressure, thus,

$$D = \frac{\alpha}{p_o}$$

If experimental data will verify that ($Ns \frac{ds}{dt}$) is small with respect to 1, the foregoing equations may be simplified and integrated to give drying times directly. Further, for a temperature difference of 100^{o} F between the exterior surface and the subliming interface, the exponential term approximates unity and the following results may be obtained for the drying time T_o of a slab at thickness S_o.

(a) Diffusion regime

$$t_o = \frac{S_o^2}{2\left\{1 + \sqrt{1 + M\left(\frac{p_i - p_{wo}}{p_o}\right)}\right\}}$$

(b) Combined diffusion and hydrodynamic continuum regime

$$t_o = \frac{S_o^2}{2\left\{1 + \sqrt{1 + M\left(\frac{p_i - p_{wo}}{p_o}\right) + \frac{a}{32}\varphi(p_i^2 - p_o^2)}\right\}}$$

(c) Hydrodynamic slip flow regime

$$t_o = \frac{S_o^2}{2\left\{1 + \sqrt{1 + \left(\frac{a}{32} + \frac{4}{3}\sqrt{\frac{2}{\pi}}\lambda z\right)\varphi(p_i^2 - p_o^2)}\right\}}$$

(d) Hydrodynamic free molecule flow regime

$$t_o = \frac{S_o^2}{2\left\{1 + \sqrt{1 + \frac{4}{3}\sqrt{\frac{2}{\pi}}\lambda\varphi(p_i^2 - p_o^2)}\right\}}$$

The respective regimes have been chosen in the order in which they may be expected to occur with decreasing total pressure. It is interesting that this analysis agress with the observation made by Harper and Tappel (18) that drying times are proportional to the square of the thickness. The results also indicate that drying times may be progressively shortened by decreasing the total pressure. It is important to note that for low total pressures, the total pressure is approximately equal to the vapor pressure and hence governed by the condenser system.

Experiment will be necessary to verify the validity of the assumed drying regimes and to delineate the ranges of total pressure in which each is valid. Experiment is also necessary to extend the data on the properties of frozen and dried foodstuffs.

3.4 EXPERIMENTAL INVESTIGATION

3.4.1 Apparatus and instrumentation

Transient temperature and pressure distributions during the freeze drying of meat can be measured with the equipment shown in Fig. 9. Samples are placed in a drying cabinet which is a two-foot steel cube and is evacuated by a 30 cfm compound mechanical vacuum pump. A trap type condenser containing dry ice and acetone is placed between the cabinet and the pump. This apparatus provides good conditions for vapor flow so that only a small pressure difference exists between the sample and the condenser. Heat is radiated to the meat from an electrically heated panel located near the top of the cabinet. The panel is coated with a substance of known emissivity so that accurate heat transfer calculations may be made.

Because of the very slow rate of drying, it is necessary to use samples that are less than two inches thick. As a result, it is necessary to use very small pressure and temperature probes so that they will have a minimal effect on the process. Therefore, the temperature probes are fine thermocouples which are threaded through the meat with a long needle. The output of each thermocouple is measured with a potentiometer. The pressure probes are made of hypodermic tubing and are connected to a manifold which in turn is connected to an alphatron vacuum gauge as shown in Fig. 9. The pressure sensing circuit is designed for minimum volume. To minimize the response time of the pressure circuit, the lowest pressure is recorded first so that each measurement will "come up" to the reading. Both the pressure and temperature probes are installed in the samples before freezing.

3.4.2 Preparation of samples

The samples are carefully cut to preserve a uniform grain direction

from top to bottom and to insure essentially one dimensional drying with the subliming interface remaining almost plane. The direction of the fibers and fatty inclusions have a marked effect on the rate and direction of drying. Obtaining a sample of significant size and uniform grain direction is not a well defined technique. However, the combination of aluminum foil shielding and judicious cutting of the sample yields a one-dimensional freeze-drying situation, without resorting to outsized samples or using excess meat for thermal guarding at the sides.

Dissection of samples after drying reveals no deleterious effects on the drying process caused by the thermocouples immersed in the product. No local melting or drying is detected along the paths of the thermocouple wires.

There is little indication that the pressure probes markedly affect the drying process. Dissection of samples after partial drying reveals no local drying or melting around the probe heads. However, some local drying to a depth of approximately 1/4 inch is found around the tubes at the outside surface of the sample. Evidently, the probes conduct heat part way into the product and provide a path around their outer surfaces for the vapor efflux. This result clearly sets a lower limit to the probe immersion depth.

3.4.3 Temperature and pressure distribution

The transient temperature distribution during freeze drying is given in Fig. 10. The heater temperature remained close to 210° F during the entire experiment; the chamber pressure remained close to 100 microns. The position of pressure probes used to measure the transient pressure distribution throughout the sample is given in Fig. 11. The pressure distribution is given in Figs. 12 and 13.

The reliability of the pressure measurements is questionable. The inconsistencies are attributed to two factors. First, condensate becomes entrained in the probes and connecting lines during transfer of the meat samples from the freezer to the dryer. Without extensive pumping of the probe lines, it is difficult to be sure that one is not reading the vapor pressure of the condensate at some unknown temperature.

Second, each probe line and the manifold had to achieve pressure equilibrium for each reading. Because the system approaches this equilibrium very slowly, a slight leak in the manifold or exterior lines could mask the stabilization to a degree that almost any reading could be obtained at any station. A solution to the above difficulties would be to replace the present system of valves which are used to permit one vacuum gauge to measure pressures at many points. By replacing this system with a system employing a separate vacuum gauge for each position that the pressure is measured, the accuracy will be improved considerably. It also would seem advisable to provide a means to pump out the probes and sensing heads after the probes are frozen in the sample

Due to experimental difficulties, it was not possible to obtain sufficiently accurate pressure measurements to warrant a detailed analysis of the data. It is expected, however, that this work will be continued in the future, and that accurate experimental measurements will be made.

REFERENCES

1. Schmidt, E. "Heat Radiation of Technical Surfaces at Ordinary Temperature". BEIHEFTE ZUM GESUNDHEITS-INGENIUR, 1, 20, 1927.

2. Buckley, H. "On Radiation from Inside of a Circular Cylinder". PHIL. MAG, 17, 576, 1937.

3. Daws, L. F. "The Emissivity of a Groove". BRIT. JR. APPL. PHYS. 5, 182, 1954.

4. Rossman, M. G. "Radiation from a Hollow Cylinder". BRIT. JR. APPL. PHYS., 6, 262, 1955.

5. Snyder, N. W., J. T. Gier, and R. V. Dunkle. "Total Normal Emissivity Measurements on Aircraft Materials between 100° and 800° F". TRANS. AM. SOC. MECH. ENG., 77, 1011, 1955.

6. McAdams, W. H. HEAT TRANSMISSION. McGraw Hill, 476, 1954.

7. Kline, S. J. and F. A. McClintock. "Describing Uncertainties in Single Sample Experiments". MECH. ENG., 75, 3, 1953.

8. Awbery, J. H. and E. Griffiths. "Thermal Properties of Meat". JR. SOC. CHEM. IND. 52, 326, 1933.

9. Hardy, J. D. and G. F. Soderstrom. "Heat Loss from the Nude Body and Peripheral Blood Flow at 22-35°C". JR. NUTRITION 16, 493, 1938.

10. Tappel, A. L., A. Conroy, M. R. Emerson, L. W. Regier and G. F. Steward. "Freeze Dried Meats, Preparations and Properties". FOOD TECH, 9, p. 401, 1955.

11. Cherneeva, L. I. "Study of the Thermal Properties of Foodstuffs". (Report of VNIKHI) Gostorgisdat, Moscow, 16 pages, 1956.

12. Harper, J. C. and C. O. Chichester. "Micro-wave Spectra and Physical Characteristics of Fruit and Animal Products Relative to Freeze-dehydration". FINAL REPORT, Contract No. DA 19-129-QM-1349, University of California Agricultural Engineering and Food Technology Departments, Davis, California, 1960.

13. Lentz, C. P. "Thermal Conductivity of Meats, Fats, Gelatin Gels, and Ice". FOOD TECH. 15 No. 5 Page 243, 1961.

14. Miller, H. L. THE MEASUREMENT OF THERMAL CONDUCTIVITY OF BEEF. M.S. Thesis. Northwestern University, Evanston, Illinois, 1961.

15. ASTM Designation C177-45T. "Method of Test for Thermal Conductivity of Materials by Means of a Guarded Hot Plate". BOOK OF ASTM STANDARDS Part 3, Page 1084, 1955.

16. Woodside, W. and A. G. Wilson. "Unbalance Errors in Guarded Hot Plate Measurements". ASTM SPECIAL TECHNICAL PUBLICATION NO. 217, p. 32, 1957.

17. Long, R. A. K. "Some Thermodynamic Properties of Fish and their Effect on the Rate of Freezing". JR. SC. FOOD AGR. 6, p. 621, 1955.

18. Harper, J. C. and A. L. Tappel. "Freeze-Drying of Foodstuffs". ADVANCES IN FOOD RESEARCH. Vol. 7, Adademic Press, 1957.

19. Luyet, B. J. American Foundation for Biological Research, "Report 1", Quartermaster Corps Food and Container Institute, September, 1959.

20. Glaser, H. "Thermal Conductivity and Diffusion of Water Vapor in Insulating Materials". KALTETECHNICK 10, March, 1958.

21. Scheideggar, A. E. THE PHYSICS OF FLOW THROUGH POROUS MEDIA. Macmillan, P. 68, 1957.

22. Jakob, M., HEAT TRANSFER. 1, Wiley, 1949.

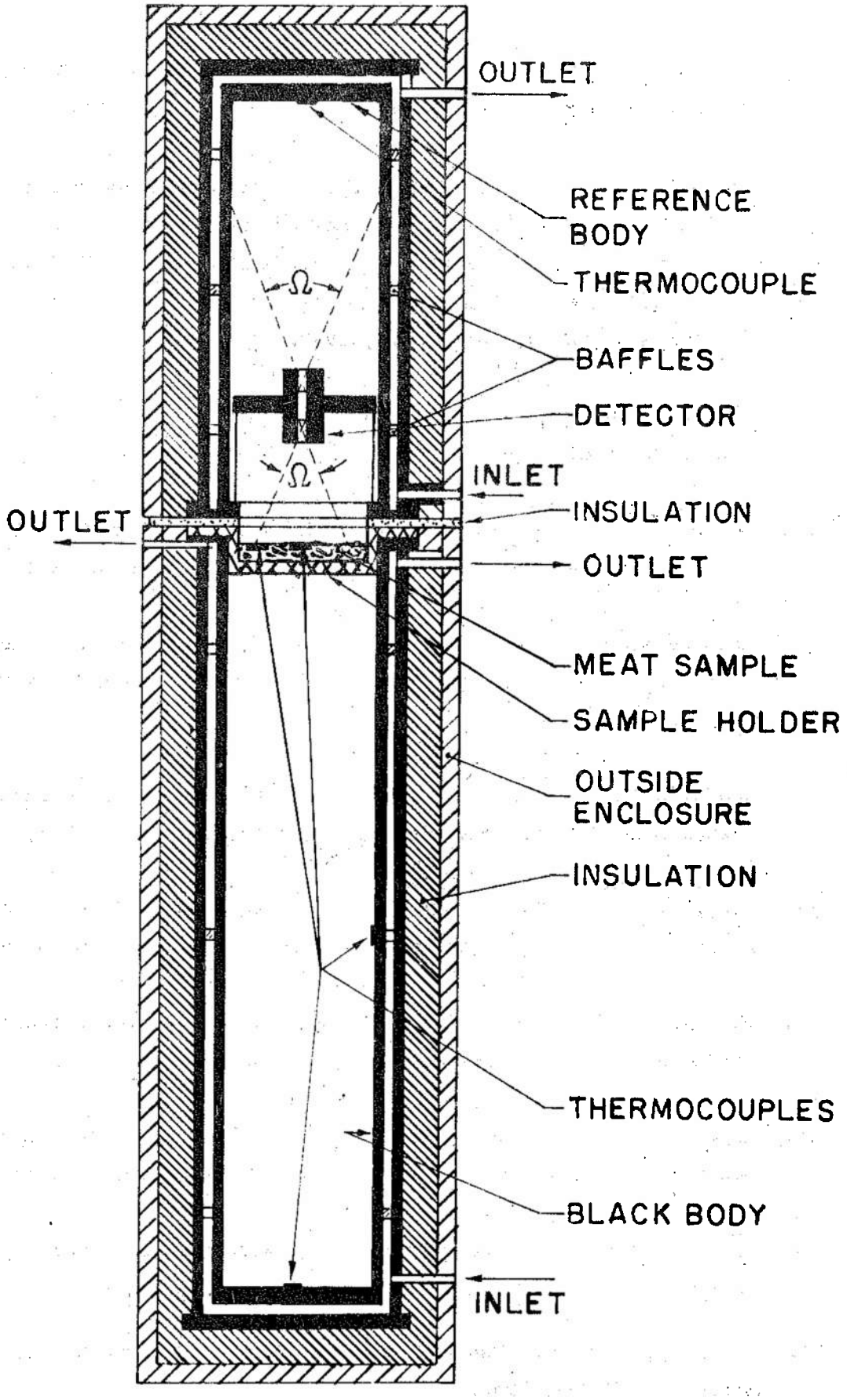

FIGURE 1. APPARATUS FOR MEASURING NORMAL EMISSIVITY

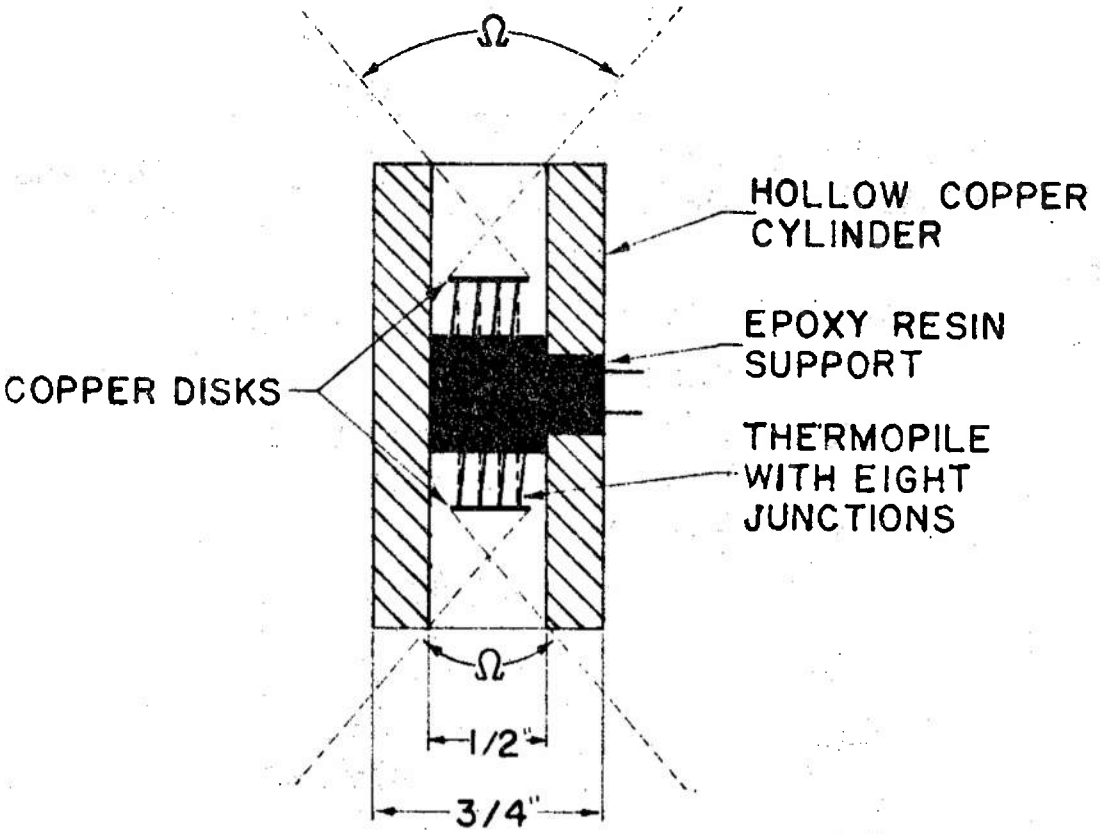

FIGURE 2. DETECTOR

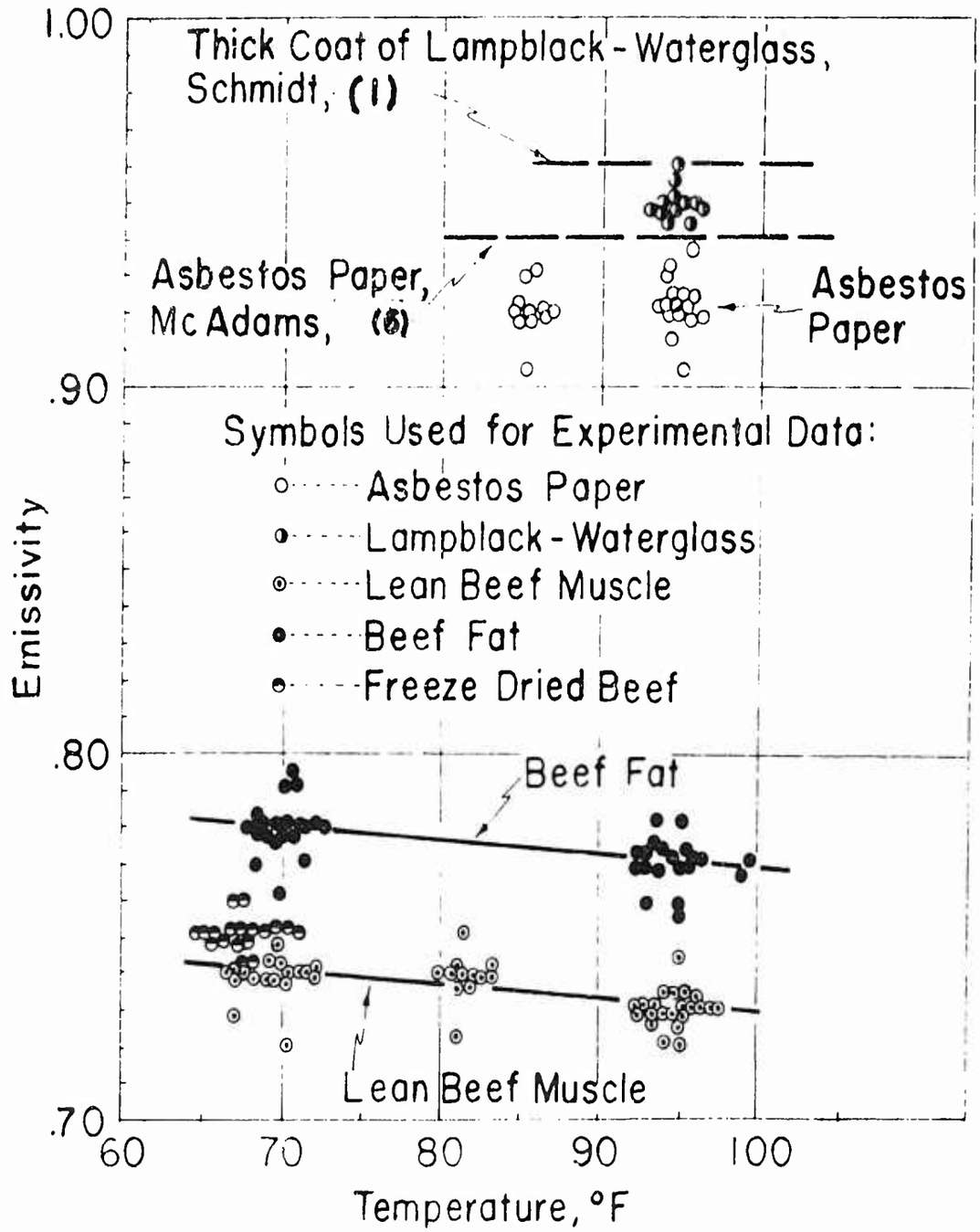

FIGURE 3. EMISSIVITY AS A FUNCTION OF TEMPERATURE

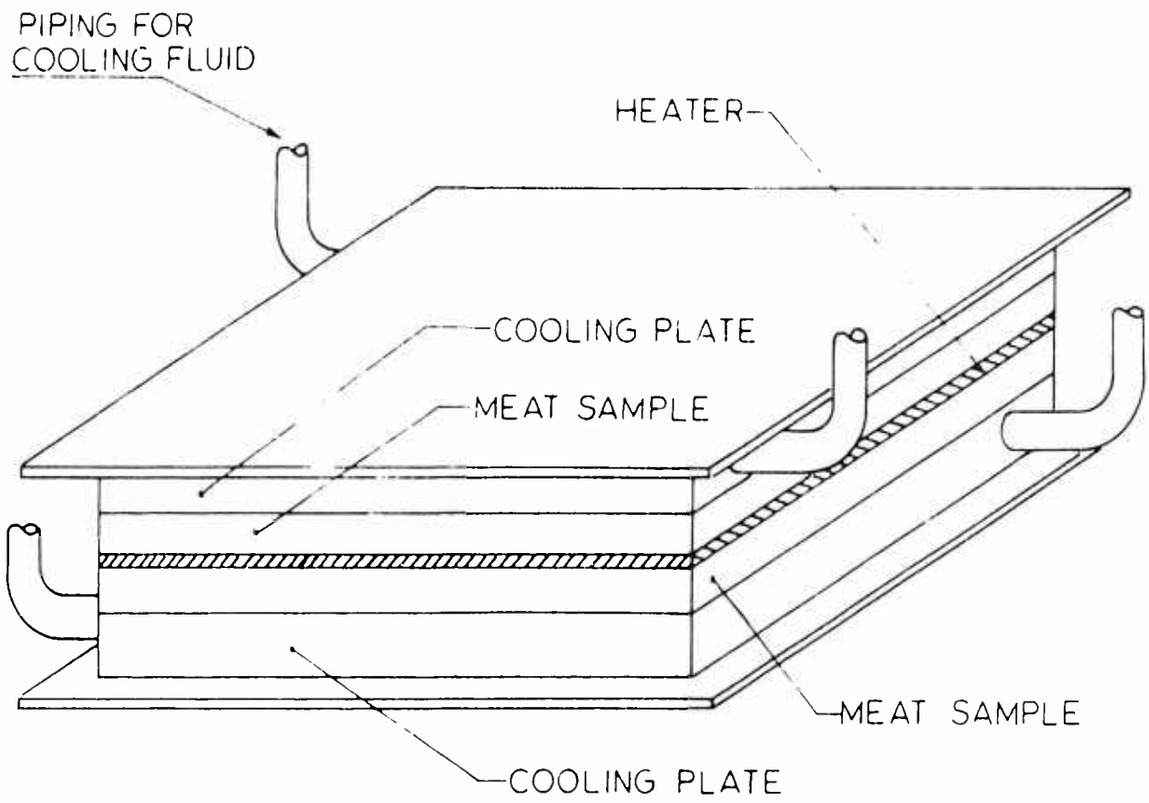

HOT PLATE ASSEMBLY

FIGURE 4

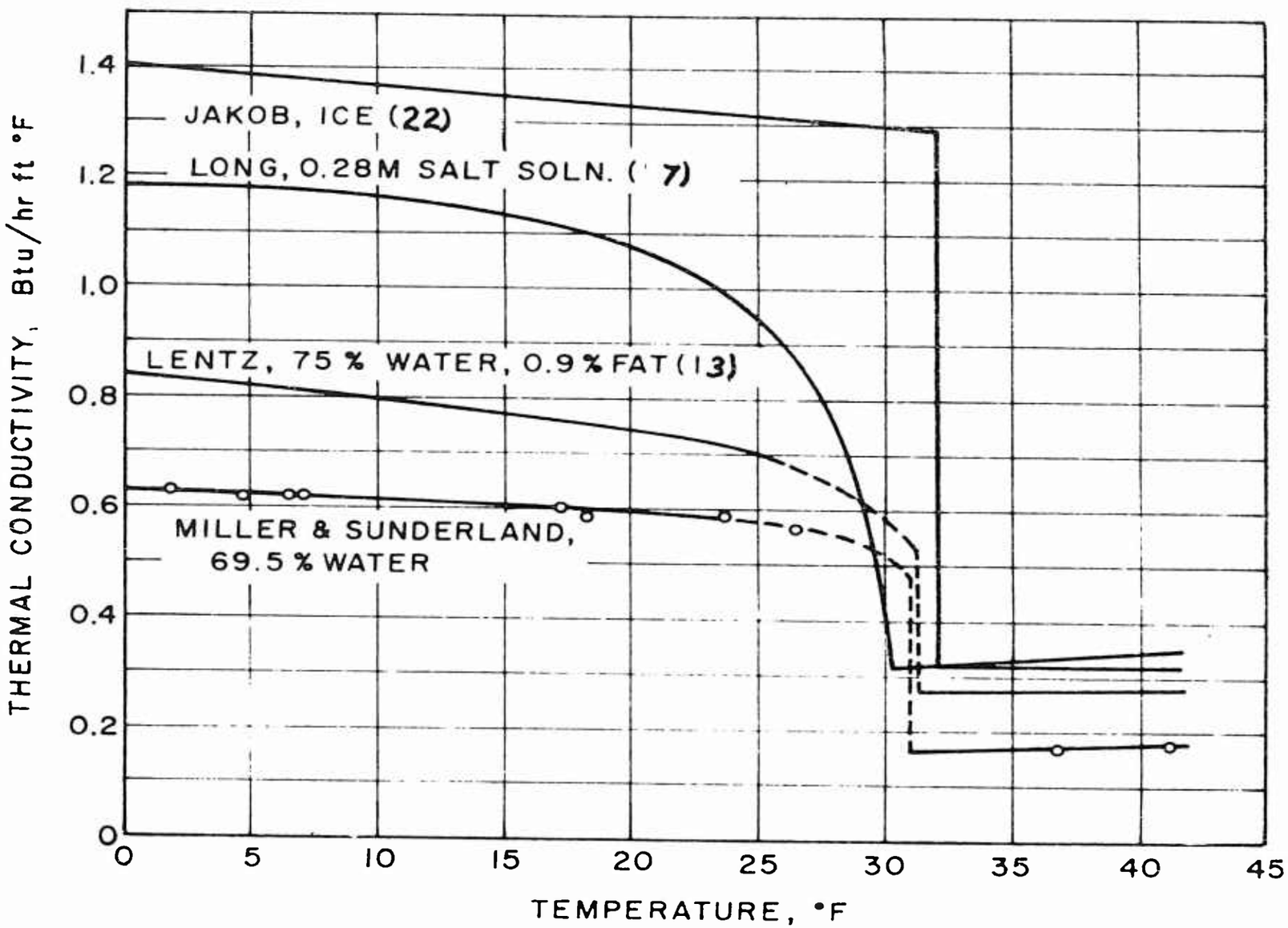

FIGURE 5. THERMAL CONDUCTIVITY OF BEEF PARALLEL TO GRAIN

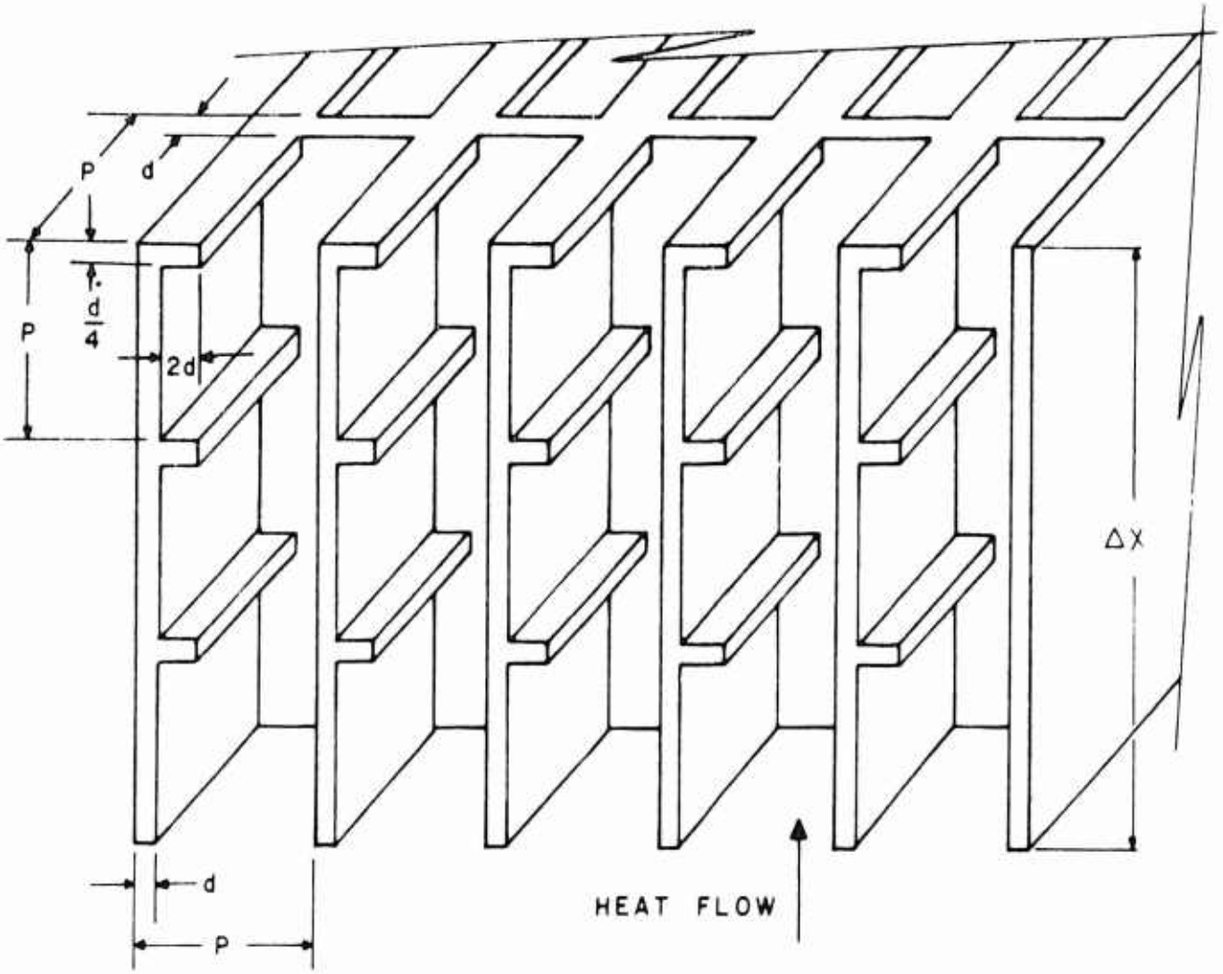

FIG. 6 . ONE DIMENSIONAL THERMAL CONDUCTIVITY MODEL FOR MEAT

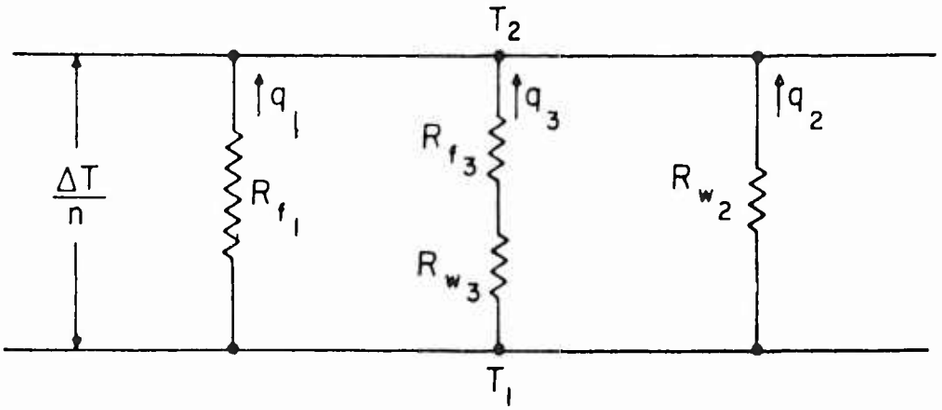

FIG. 7 . ANALOG OF HEAT FLOW PATHS THROUGH STRUCTURAL MODEL FOR MEAT

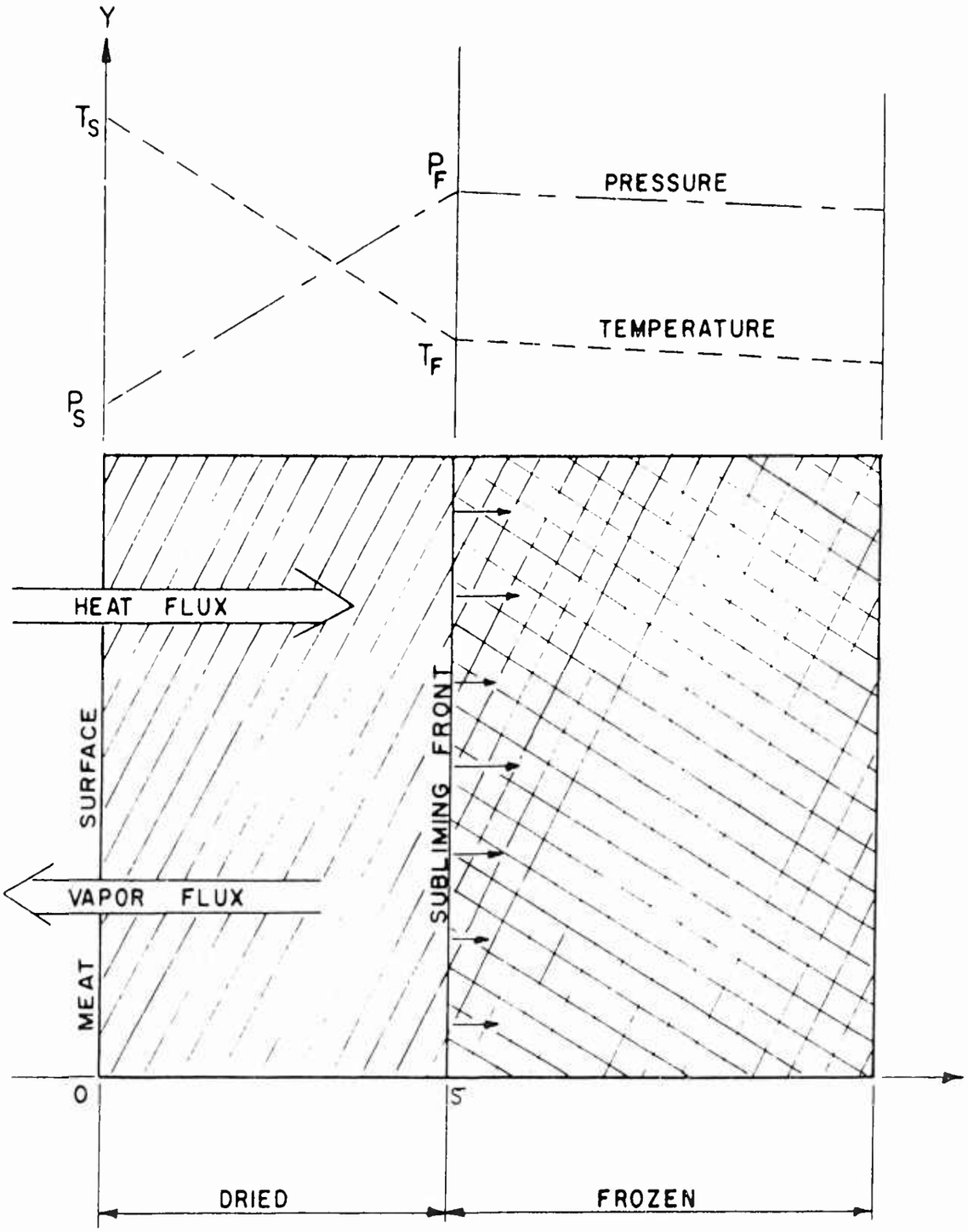

ONE-DIMENSIONAL FREEZE-DRYING
WITH RADIANT HEAT ADDITION

FIGURE 8.

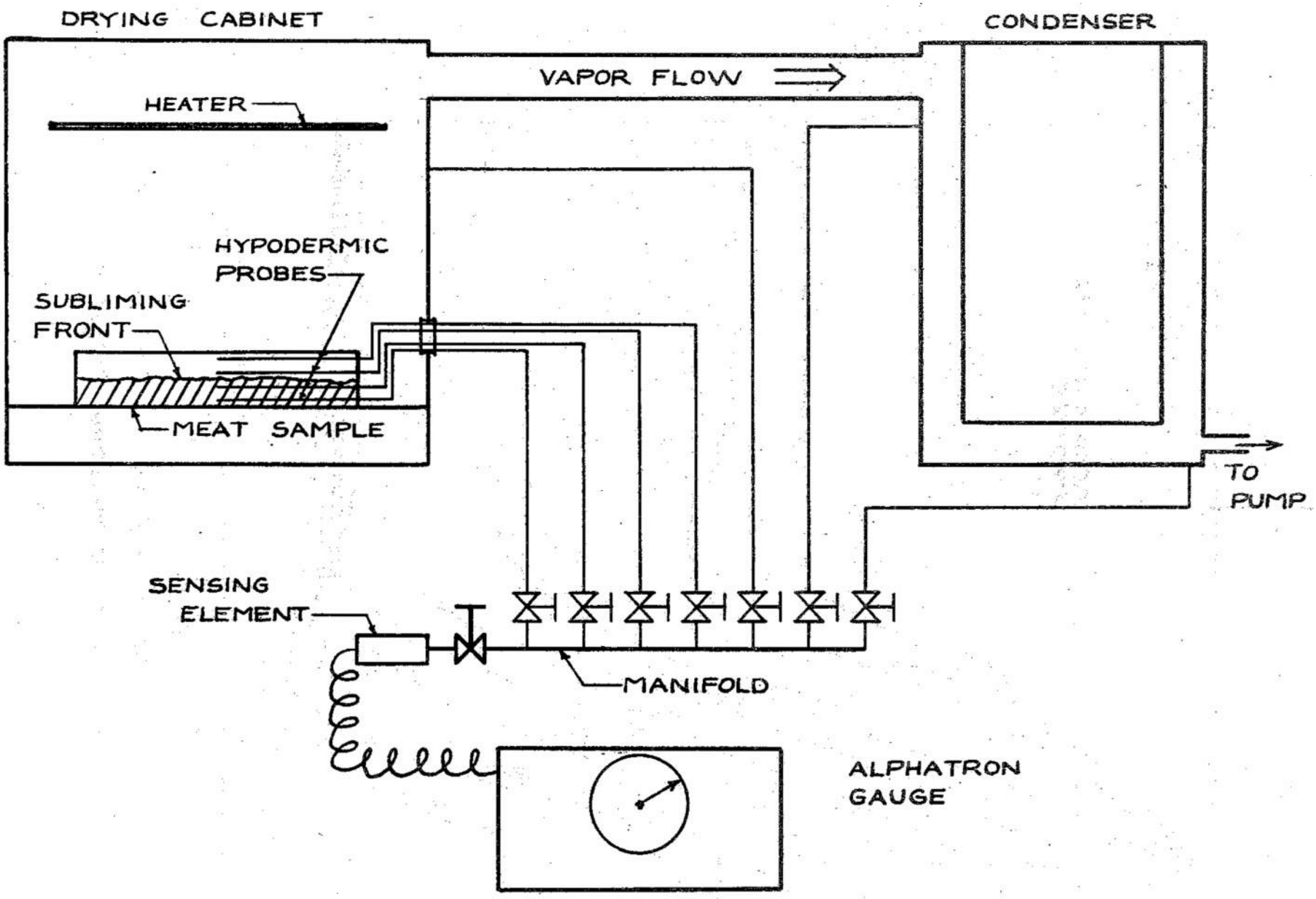

SCHEMATIC PRESSURE MEASURING LAYOUT

FIGURE 9.

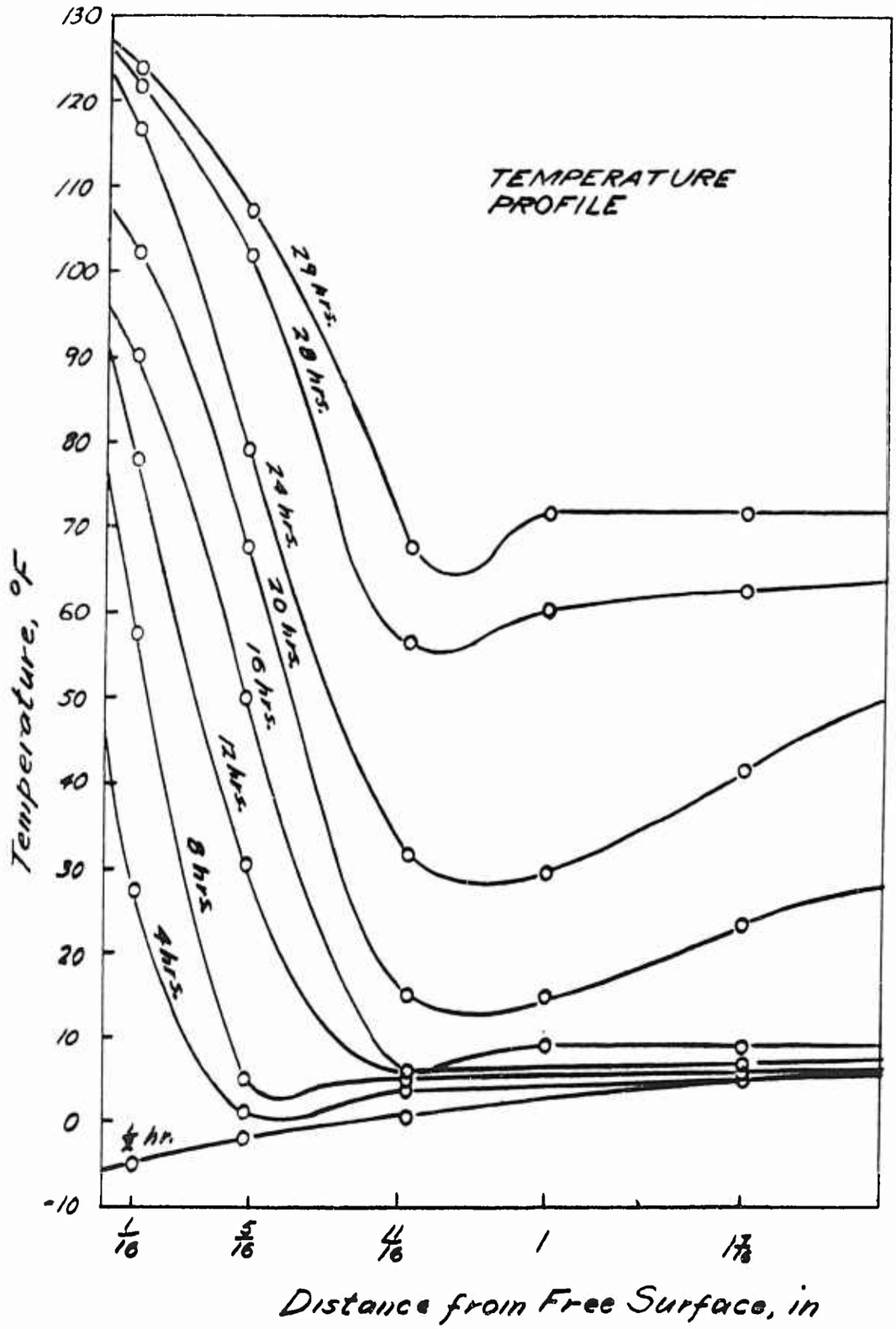

FIGURE 10. TRANSIENT TEMPERATURE DISTRIBUTION

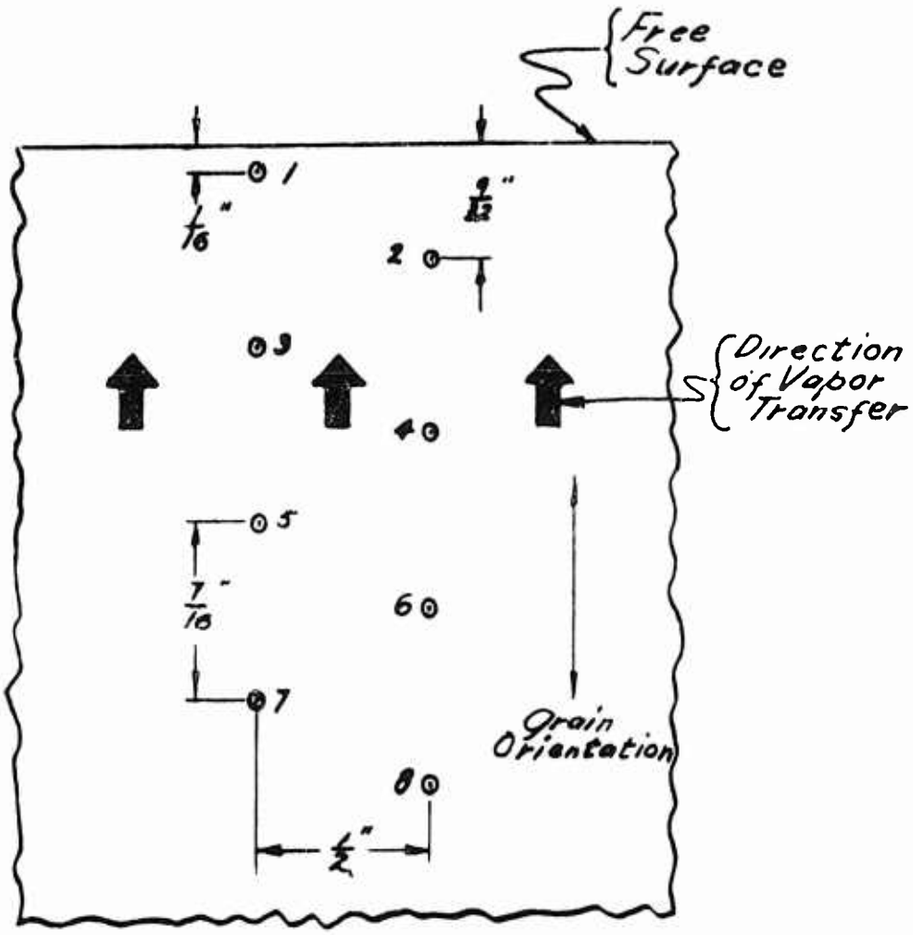

FIGURE 11. PROBE ORIFICE ARRANGEMENT WITHIN SAMPLE

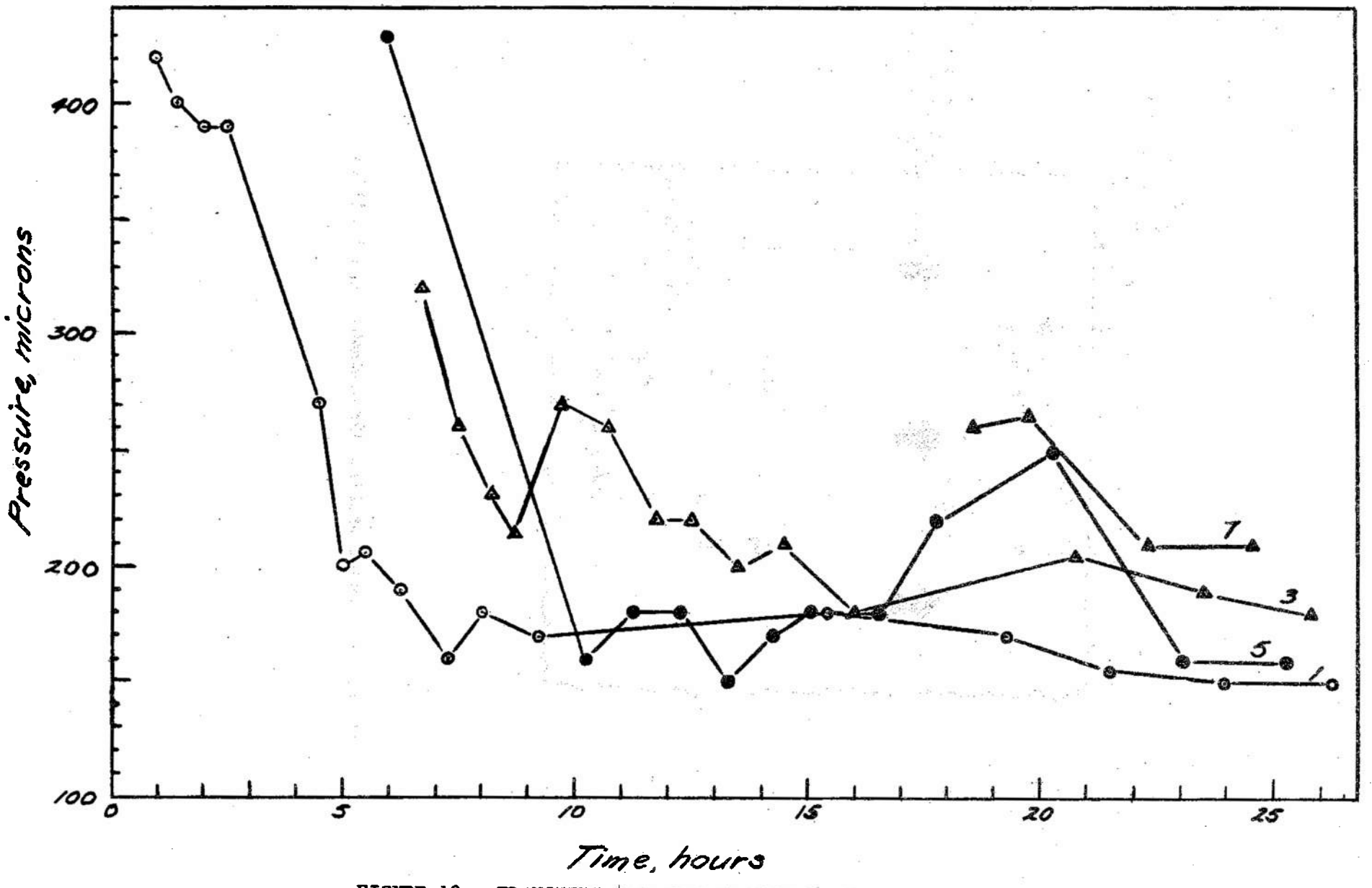

FIGURE 12. TRANSIENT PRESSURE DISTRIBUTION

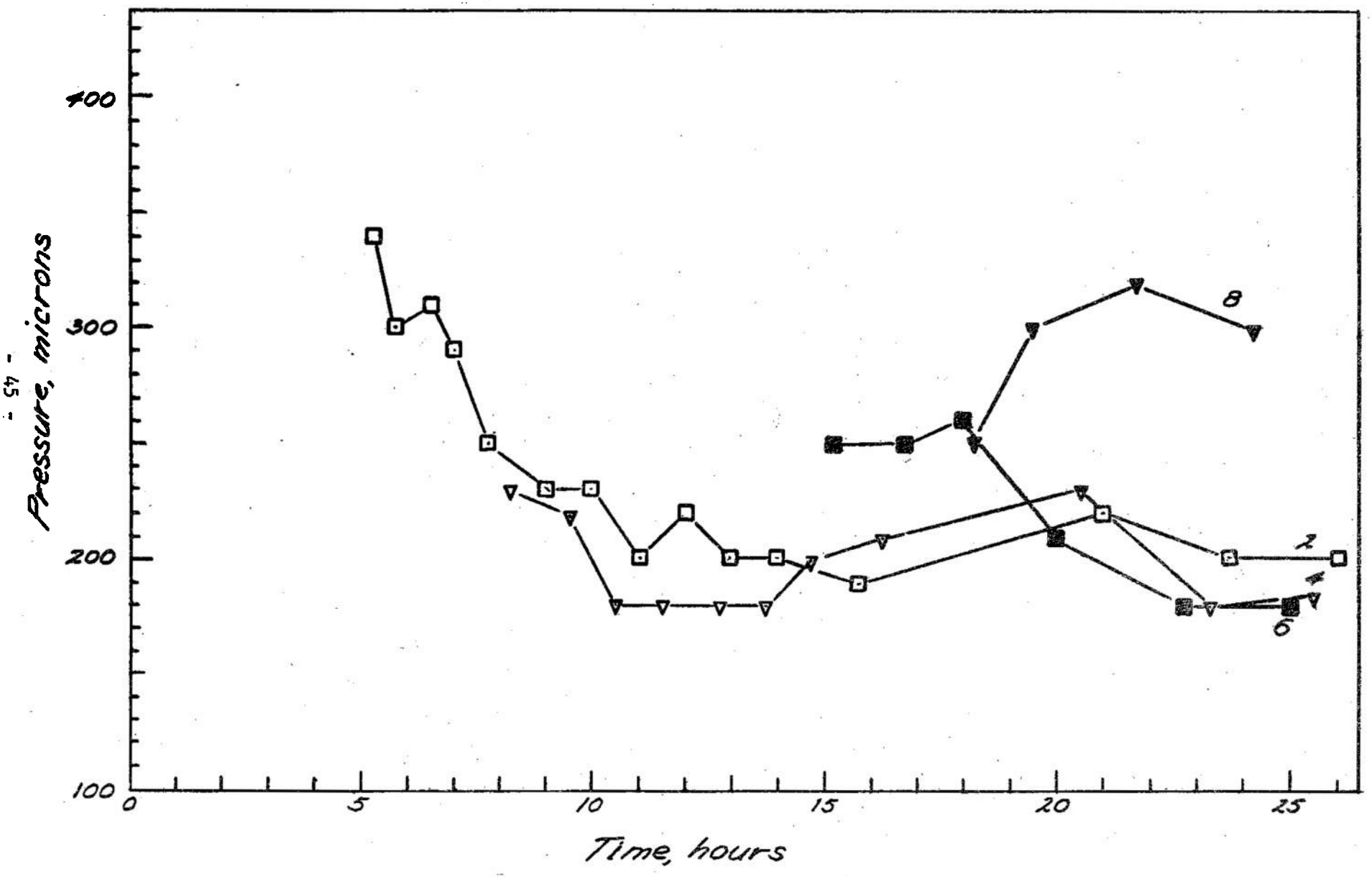

FIGURE 13. TRANSIENT PRESSURE DISTRIBUTION

AD_____Accession No._____

Northwestern University
Evanston, Illinois

INVESTIGATION INTO THE MECHANISM OF
FREEZE DRYING - J. Edward Sunderland

Final Technical Report, 28 February 1962
45 pages (Contract DA 19-129-QM-1487)
Project No. 7-84-06-032, unclassified
report. Final results are given of measure-
ments of the emissivity and thermal conductivity
of beef and studies are given concerning the
mechanism of freeze drying.

UNCLASSIFIED

1. Mechanism of freeze drying

2. Contract DA 19-129-QM-14

AD_____Accession No._____

Northwestern University
Evanston, Illinois

INVESTIGATION INTO THE MECHANISM OF
FREEZE DRYING - J. Edward Sunderland

Final Technical Report, 28 February 1962
45 pages (Contract DA 19-129-QM-1487)
Project No. 7-84-06-032, unclassified
report. Final results are given of measure-
ments of the emissivity and thermal conductivity
of beef and studies are given concerning the
mechanism of freeze drying.

UNCLASSIFIED

1. Mechanism of freeze drying

2. Contract DA 19-129-QM-14

AD_____Accession No._____

Northwestern University
Evanston, Illinois

INVESTIGATION INTO THE MECHANISM OF
FREEZE DRYING - J. Edward Sunderland

Final Technical Report, 28 February 1962
45 pages (Contract DA 19-129-QM-1487)
Project No. 7-84-06-032, unclassified
report. Final results are given of measure-
ments of the emissivity and thermal conductivity
of beef and studies are given concerning the
mechanism of freeze drying.

UNCLASSIFIED

1. Mechanism of freeze dry

2. Contract DA 19-129-

AD_____Accession No._____

Northwestern University
Evanston, Illinois

INVESTIGATION INTO THE MECHANISM OF
FREEZE DRYING - J. Edward Sunderland

Final Technical Report, 28 February 1962
45 pages (Contract DA 19-129-QM-1487)
Project No. 7-84-06-032, unclassified
report. Final results are given of measure-
ments of the emissivity and thermal conductivity
of beef and studies are given concerning the
mechanism of freeze drying.

UNCLASSIFIED

1. Mechanism of freeze dry

2. Contract DA 19-129-

AD_____Accession No._____

Northwestern University
Evanston, Illinois

INVESTIGATION INTO THE MECHANISM OF FREEZE DRYING - J. Edward Sunderland

Final Technical Report, 28 February 1962
45 pages (Contract DA 19-129-QM-1487)
Project No. 7-84-06-032, unclassified report. Final results are given of measurements of the emissivity and thermal conductivity of beef and studies are given concerning the mechanism of freeze drying.

UNCLASSIFIED

1. Mechanism of freeze drying
2. Contract DA 19-129-QM-14[illegible]

AD_____Accession No._____

Northwestern University
Evanston, Illinois

INVESTIGATION INTO THE MECHANISM OF FREEZE DRYING - J. Edward Sunderland

Final Technical Report, 28 February 1962
45 pages (Contract DA 19-129-QM-1487)
Project No. 7-84-06-032, unclassified report. Final results are given of measurements of the emissivity and thermal conductivity of beef and studies are given concerning the mechanism of freeze drying.

UNCLASSIFIED

1. Mechanism of freeze drying
2. Contract DA 19-129-QM-14[illegible]

AD_____Accession No._____

Northwestern University
Evanston, Illinois

INVESTIGATION INTO THE MECHANISM OF FREEZE DRYING - J. Edward Sunderland

Final Technical Report, 28 February 1962
45 pages (Contract DA 19-129-QM-1487)
Project No. 7-84-06-032, unclassified report. Final results are given of measurements of the emissivity and thermal conductivity of beef and studies are given concerning the mechanism of freeze drying.

UNCLASSIFIED

1. Mechanism of freeze dr
2. Contract DA 19-129

AD_____Accession No._____

Northwestern University
Evanston, Illinois

INVESTIGATION INTO THE MECHANISM OF FREEZE DRYING - J. Edward Sunderland

Final Technical Report, 28 February 1962
45 pages (Contract DA 19-129-QM-1487)
Project No. 7-84-06-032, unclassified report. Final results are given of measurements of the emissivity and thermal conductivity of beef and studies are given concerning the mechanism of freeze drying.

UNCLASSIFIED

1. Mechanism of freeze dr
2. Contract DA 19-129